Eleonora Cavallari,[a] Carla Carrera,[a] Silvio Aime,[a] Francesca Reineri[a]

Studies to enhance the hyperpolarization level in PHIP-SAH-produced C13-pyruvate

J. Magnetic Resonance, 2018, 289 12–17

https://doi.org/10.1016/j.jmr.2018.01.019

Studies to enhance the hyperpolarization level in PHIP-SAH-produced C13-pyruvate

Eleonora Cavallari,[a] Carla Carrera,[a] Silvio Aime,[a] Francesca Reineri[a]

[a] *Dept. Molecular Biotechnology and Health Sciences, Via Nizza 52, Torino, Italy*

**Corresponding author. e-mail address:* francesca.reineri@unito.it *(Francesca Reineri)*

Abstract. The use of [1-^{13}C]pyruvate, hyperpolarized by dissolution-Dynamic Nuclear Polarization (d-DNP), in *in vivo* metabolic studies has developed quickly, thanks to the imaging probe's diagnostic relevance. Nevertheless, the cost of a d-DNP polarizer is quite high and the speed of hyperpolarization process is relatively slow, meaning that its use is limited to few research laboratories. ParaHydrogen Induced Polarization Side Arm Hydrogenation (PHIP-SAH) [Reineri F.et al. 2015] is a cost effective and easy-to-handle method that produces ^{13}C-MR hyperpolarization in [1-^{13}C]pyruvate and other metabolites. This work aims to identify the main determinants of the hyperpolarization levels observed in C13-pyruvate using this method. By dissecting the various steps of the PHIP-SAH procedure, it has been possible to assess the role of several experimental parameters whose optimization must be pursued if this method is to be made suitable for future translational steps. The search for possible solutions has led to improvements in the polarization of sodium [1-^{13}C]pyruvate from 2% to 5%. Moreover, these results suggest that observed polarization levels could be increased considerably by an automatized procedure which would reduce the time required for the work-up passages that are currently carried out manually. The results reported herein mean that the attainment of polarization levels suitable for the metabolic imaging applications of these hyperpolarized substrates show significant promise.

Keywords Magnetic Resonance Spectroscopy; MR-Imaging; Hyperpolarization; ParaHydrogen; Pyruvate.

Introduction

ParaHydrogen Induced Polarization (PHIP)[1–3] is a cheap and easy-to-handle hyperpolarization method that can provide ≥ 20% hyperpolarization of ^{13}C MR signals in several substrates [4–6] in a few seconds. Although some *in vivo* studies have already been carried out [6–9], the use of parahydrogen-polarized molecules for clinical translation is still widely unexplored.

Conversely, the use of d-DNP polarized substrates [10] has proven to be a powerful imaging tool as it has produced several HP substrates that are suitable for the investigation of metabolic processes *in vivo*, in real time [11–13]. In particular, d-DNP polarized [1-^{13}C]pyruvate has been used for the study of metabolic processes in tumours [14], the heart [15,16] and in ischemic strokes [17]. D-DNP has the drawback of requiring a quite sophisticated and expensive polarizer, limiting its use to few research laboratories.

PHIP is obtained *via* the hydrogenation, using para-enriched hydrogen (hereafter named *para*hydrogenation), of suitable de-hydrogenated precursors of target hyperpolarized molecules. The parahydrogen hyperpolarization of some of the most important metabolic imaging reporters, above all pyruvate, therefore only became possible after the recent introduction of the Side Arm Hydrogenation (PHIP-SAH) strategy [18]. In this method, hyperpolarized [1-^{13}C]pyruvate and other carboxylate containing molecules [19], are produced *via*: 1) the esterification of the carboxylate group with an unsaturated alcohol (e.g. propargyl alcohol, vinyl alcohol) [20]; 2) the *para*hydrogenation of the ester derivative, 3) the spin order transfer from the parahydrogen protons to the ^{13}C carboxylate spin and 4) ester hydrolysis (Scheme 1). The polarization transfer step has been studied and a variety of methods for the PHIP hyperpolarization of heteronuclei have been reported [21,22]. These methods are based on pulse sequences [23–26], or magnetic field cycling (MFC) [27]. It has been reported that pulse sequence based polarization transfer methods, which are often used with PHIP polarizers [28–30], are less efficient than MFC because small, long-range J couplings are involved [31]. However, it is worth noting that a recent study [32] has shown that the PH-INEPT+ sequence provides efficient polarization transfer despites exploiting small J-couplings [26].

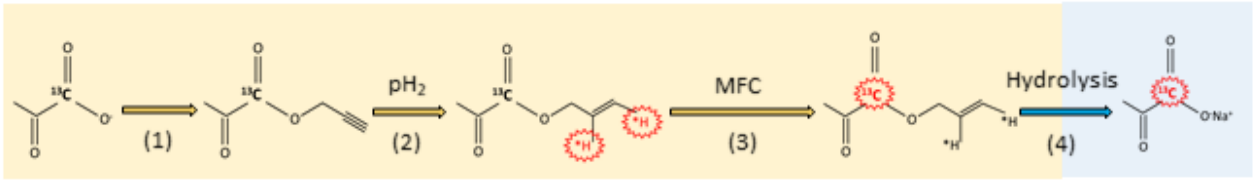

Scheme 1. Diagram of the PHIP-SAH procedure: 1) functionalization of the carboxylate group with the side-arm; 2) *para*hydrogenation of the unsaturated alcohol; 3) transfer of parahydrogen spin order to the ^{13}C spin of the carboxylate group; 4) cleavage of the side-arm. The yellow background indicates that steps take place in the organic phase, while the blue background indicates that the molecule is dissolved in the water phase.

The polarization level of the end product can be increased *via* the optimization of the following steps: the *para*hydrogenation reaction, the polarization transfer and hydrolysis of the ester. In the present work, propargyl-pyruvate has been used as an unsaturated precursor of hyperpolarized [1-^{13}C]-pyruvate.

Hyperpolarization level depends on 1) the percentage of hydrogen para-enrichment and the mandatory requirement that the hydrogen molecule is added to the unsaturated substrate in a pairwise manner; 2) the efficiency of the polarization transfer step from ^{1}H to ^{13}C, performed here by MFC and 3) polarization losses that occur during the hydrolysis and phase transfer of the ^{13}C labelled product from the organic solvent. It must be reminded that mixing between *para*- and *ortho*- states on reaction intermediates must be limited as much as possible and, in the ideal case, the singlet state of parahydrogen might be transferred to the product purely [3].

We herein report a study that aims to enhance the [1-^{13}C]pyruvate polarization level from the 2% value that was obtained when the PHIP-SAH method was initially conceived [31].

Experimental methods

Parahydrogen enrichment measurements

The ^{1}H-NMR spectra of hydrogen gas were acquired using 5mm NMR tubes equipped with PTFE gas valves. The NMR tubes were filled with 2 bar of hydrogen at room-temperature equilibrium (25% para-enriched), or parahydrogen (92% para-enrichment). Para-enrichment was quantified using ^{1}H-NMR spectra acquired at 14.1T [33].

Parahydrogen (92% para-enrichment) was generated by flowing room temperature hydrogen gas (electrolysis, FDGS WM-H2) through a chamber with a conversion catalyst at 36 K (Bruker BPHG). Para-enrichment was found to be 90±2% as observed by ^{1}H-NMR spectroscopy at 14.1T (Bruker spectrometer) and described by Bibo et al. [33].

In order to estimate the extent of parahydrogen depletion during the parahydrogenation process, parahydrogen enrichment was measured in the gas phase after reaction completion. In order to do this, the catalyst was activated (see the following section), the substrate was added, and the NMR tube was pressurized with 92% *para* hydrogen (2bar). ^{1}H-NMR of the hydrogen gas was acquired both before and after

the reaction vessel was shaken in a hot water bath (353 K). In both cases, the hydrogenation mixture was kept at the bottom of the NMR tube, out of the MR detection coil.

Parahydrogenation reaction

The hydrogenation catalyst [1,4-bis(diphenylphosphino)butane](1,5-cyclooctadiene)rhodium(I) tetrafluoroborate ($1*10^{-3}$mmol, Sigma-Aldrich) was activated in the same NMR tube as used for the substrate hydrogenation reaction. In order to activate the catalyst, 30μl of anhydrous ethanol were added to the solid catalyst powder, the tube was pressurized with normal hydrogen (Ultra High purity grade Hydrogen, 99.999%, Praxair, 7 bar) and allowed to react overnight (about 15 hours) at 298 K. The catalyst was then dissolved and the ethanol turned dark orange. Next, the solution was frozen in a liquid nitrogen bath and 100 μl of chloroform containing $25*10^{-3}$mmol of propargyl-[1-^{13}C]pyruvate (synthesized as reported in [19]) were added. The NMR tube was frozen using liquid nitrogen, pressurized with parahydrogen (92% enrichment), and stored in a liquid nitrogen bath until the hyperpolarization experiment was started.

The NMR spectrometer (Bruker Avance 14.1T spectrometer) was prepared for the acquisition of the ^{1}H-NMR hyperpolarized spectra. Magnetic field adjustments (shimming), and frequency tuning (^{1}H and ^{13}C) were carried out on a sample that was similar to those obtained from the parahydrogenation reaction. The hyperpolarized spectra were then acquired without any adjustment being made, which lead to significant detrimental effect being observed in the ^{1}H-NMR hyperpolarized spectra (see e.g. figure 2).

In the ALTADENA-type experiment [34], the *para*hydrogenation reaction was carried out in close proximity to the NMR spectrometer, but outside of the fringe field of the magnet (magnetic field ~ 100μT). The NMR tube was heated in a water bath (353 K) for 7-8 seconds and vigorously shaken for 3 seconds before the valve was opened and 200 ul of chloroform were added in order to provide a sufficient volume for the acquisition of an NMR spectrum. The tube was quickly placed in the NMR spectrometer (20±2 s), and a ^{1}H-NMR spectrum was acquired immediately. After thermal polarization was re-established, the ^{1}H-NMR reference spectrum, which was used to quantify the ^{1}H polarization level (see S.I.) was acquired (10 min after hydrogenation). The time delay between the end of hydrogenation (i.e. chloroform addition) and ^{1}H-NMR spectrum acquisition was 20 seconds. In order to estimate the ^{1}H polarization level at time zero, i.e. immediately after

*para*hydrogenation completion, a variety of ALTADENA experiments were carried out in which the time delay between chloroform addition and the acquisition of the ^{1}H-NMR spectrum was gradually increased.

^{13}C hyperpolarization

MFC was used to transfer the spin order of added parahydrogen protons to the target ^{13}C carboxylate spin. This was done in a magnetic field shield (mu-metal triple shield), bearing a solenoid coil that was supplied with an electric current controlled by a custom-written function (the whole device was provided by Aspect Imaging). In the experimental procedure, the NMR tube was placed in the mu-metal shield immediately after shaking. The sample was then lifted out of the mu-metal box, chloroform was added and the ^{13}C-NMR spectrum acquired in the shortest possible time (~30 seconds between the end of MFC and the acquisition of the ^{13}C-NMR spectrum).

The thermally polarized ^{13}C-NMR spectrum was acquired 15 min after hydrogenation (8 transients, repetition time 200 s). ^{13}C polarization was calculated as reported in S.I., each experiment was repeated three times.

Nascent ^{13}C polarization, i.e. polarization occurring immediately after MFC, was estimated by back calculation having carried out the ^{13}C hyperpolarization experiment on a number of samples, with increasing delays between the end of MFC and ^{13}C-NMR spectrum acquisition. During these intervals, the samples were kept at earth's field, while the time spent in the NMR spectrometer remained constant.

Hydrolysis

In the first set of experiments, hydrolysis was carried out, as reported below, using an aqueous sodium hydroxide solution (0.1M). Sodium ascorbate (0.05 M) was added to the base solution in later experiments. The aqueous base was heated to 353 K and pressurized with inert gas (Ar, 3bar) in order to facilitate the quick and efficient mixing of the aqueous and organic phases. After the hydrogenation reaction and the application of MFC, the NMR tube was opened and the aqueous base was injected into the organic phase. An acidic buffer (HEPES, 100 ul,144mM, pH5.4) was added a few seconds (4-5s) later. Finally, the aqueous fraction was removed using a cannula connected to a syringe and it was transferred into a 5 mm tube for ^{13}C-NMR acquisition.

The time delay between the injection of the aqueous base and the acquisition of the ^{13}C-NMR spectrum was 40-45 seconds (see figure 1). In order to back-calculate the ^{13}C polarization to time zero, i.e. immediately after ester hydrolysis, the relaxation time of the ^{13}C carboxylate signal was estimated at earth's field. Several hydrolysis experiments were carried out on a number of samples, using increasing time delays (Δt), between the addition of the acidic buffer and the acquisition of the ^{13}C-NMR spectrum (see figure 1). The polarization decay constant and the nascent ^{13}C polarization ($P(t_0)$) were obtained from the interpolation of ^{13}C hyperpolarized signals with an exponential decay curve (see figures S3 and S4).

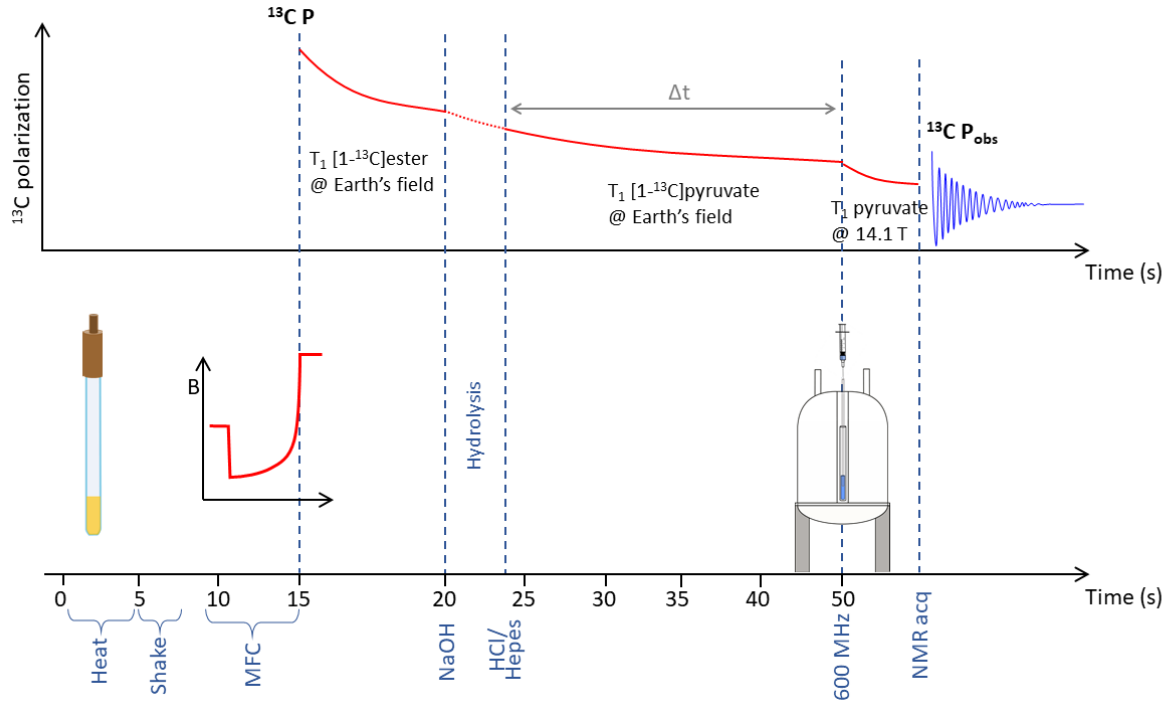

Figure 1. PHIP-SAH experimental workflow. The upper part of the figure illustrates the ^{13}C hyperpolarization process, from the end of MFC (^{13}C $P(t_0)$) to ^{13}C-NMR spectrum (^{13}C P_{obs}) acquisition. It was observed that ^{13}C polarization decays according to a variety of relaxation time constants (T_1 of the allyl ester at the earth's field, T_1 of pyruvate, after hydrolysis, at the earth's field and T_1 of pyruvate in the high field magnet). The experiment was repeated at various Δt delay times to determine the T_1 of [1-^{13}C]-pyruvate at the earth's field.

Results

^{1}H hyperpolarization assessment

Parahydrogen is non-magnetic and only the ortho-hydrogen signal can be observed by NMR. Upon comparing the ^{1}H-NMR spectra of hydrogen at room-temperature equilibrium and para-enriched (figure S1), it was

found that the hydrogenation reaction is accompanied by a dramatic decrease in the para-H_2 enrichment from 90± 2 % to 50 ± 5%.

The ^{1}H hyperpolarization level observed in the ALTADENA experiment (figure 2), is a direct readout of the efficiency of singlet state transfer to the product and was found to be 11.7 ± 0.7% on allyl-pyruvate, 20 s after the end of hydrogenation. Nascent polarization on ^{1}H-NMR signals ($P(t_0)$), which corresponds to the maximum polarization on parahydrogen protons, was estimated to be 23.9 ± 3.3 % (Figure S2).

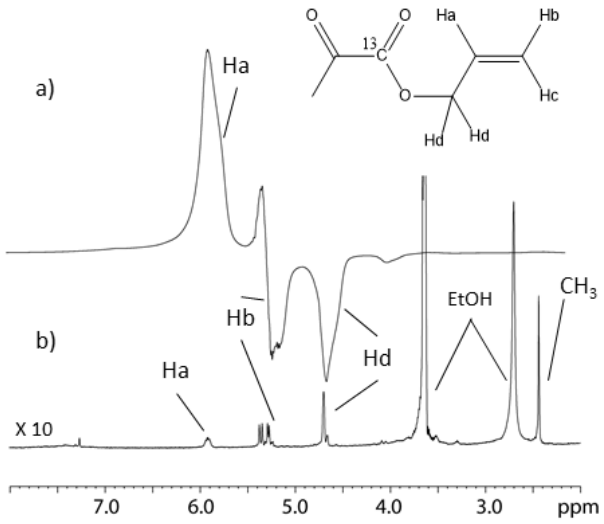

Figure 2. High field ^{1}H-NMR spectra of *para*hydrogenated allyl-pyruvate obtained in a ALTADENA experiment: a) 20 s after the addition of parahydrogen at ~100 uT (ALTADENA conditions); b) in thermal equilibrium, 10 min after hydrogenation (the spectrum was multiplied by 10). ^{1}H polarization was 11.7 ± 0.7%, see S.I. for experimental details. Magnetic field homogeneity was adjusted, before hyperpolarized spectrum acquisition (a), using a different sample and then improved before the acquisition of the thermally polarized sample (b). This leads to the significantly inferior lineshape seen in the HP spectrum compared to the thermally polarized one.

^{13}C hyperpolarization assessment

^{1}H hyperpolarization was transferred to the ^{13}C carboxylate signal by means of the MFC. The magnetic field in the shield was initially set to 1.5μT. At this field, the frequency difference between ^{1}H and ^{13}C nuclei is 48.1 Hz and weak coupling between protons and the ^{13}C carboxylate nucleus still occurs (see S.I. for J coupling values). Immediately after the placement of the *para*hydrogenated sample in the shield, the field was

dropped to 30nT in 1ms, (diabatic passage), where the frequency difference $\Delta\nu_{HC}$ is 0.95 Hz and isotropic mixing occurs between allyl group protons and the ^{13}C carboxylate, i.e. $\Delta\nu_{HC}$ is the same order of magnitude as their scalar coupling constant [31]. Finally, the magnetic field was exponentially increased to 10 μT in 4 seconds (adiabatic remagnetization).

The ^{13}C polarization observed on the ester (P_{obs}) was 8.3 ± 0.7%, which corresponds to a 6850 ± 650-fold signal enhancement with respect to thermal equilibrium, at 14 T. The delay between the end of MFC and the ^{13}C-NMR spectrum acquisition (Δt) was 30 seconds, most of which was spent at earth's magnetic field. The T_1 of the pyruvate ester ^{13}C carboxylate signal at earth's field was estimated as being 88.8 ± 12.5 seconds using Δt variation, as detailed in the experimental methods. The nascent polarization ($P(t_0)$), i.e. polarization occurring immediately after the end of MFC, was estimated to be 10.4 ± 1.0%.

Once hyperpolarization was transferred to the ^{13}C carboxylate signal, the ester was hydrolysed at earth's magnetic field to provide an aqueous solution of hyperpolarized sodium pyruvate. Following the injection of the pressurized, heated NaOH solution (0.1M), an emulsion of organic phase in aqueous base was instantaneously formed and ester hydrolysis occurred at the interface. The two phases then quickly separated (3-4 seconds). Phase separation was further improved by the addition of an acidic buffer (HEPES 144 mM, pH 5.4). Under these conditions, the maximum ^{13}C signal enhancement observed on the carboxylate signal in the aqueous phase was 2800 ± 50 at 14.1T (3.4 ± 0.05 % ^{13}C polarization). T_1 was measured at the earth's field (T_1 = 41.6 ± 2.7 s, see experimental methods) and the signal enhancement estimated before hydrolysis was 5000 ± 100 (see Figure S3). We surmise that the difference in the polarization of the ester and the aqueous pyruvate solution, can be is attributed to the paramagnetic impurities derived from catalyst degradation. This hypothesis lead us to add a radical scavenger (ascorbate 50mM), which has already been used in d-DNP experiments [35], to the aqueous base. When hydrolysis was carried out using this solution, the observed polarization level increased to 5.16 ± 0.18 % (observed S.E. 4250 ± 150) and the relaxation time constant at earth's field increased also (54.4 ± 4.4s). The nascent ^{13}C polarization (^{13}C Pol(t_0), see figure 1 and 3) was 9.45 ± 0.5 % (signal enhancement 7780 ± 400 times). This result indicates that ascorbate significantly limits polarization loss during hydrolysis.

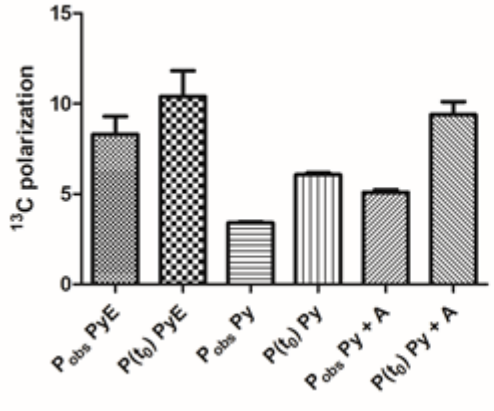

	^{13}C P_{obs}	^{13}C $P(t_0)$
Py E	8.3 ±0.7	10.4 ± 1
Py	3.4 ± 0.05	6.1 ± 0.1
Py + A	5.2 ± 0.2	9.4 ± 0.5

Figure 3. ^{13}C polarization observed (P_{obs}) and nascent ($P(t_0)$): PyE indicates allyl pyruvate (P_{obs} and $P(t_0)$); Py indicates sodium [1-^{13}C]pyruvate after hydrolysis with NaOH (without ascorbate) (P_{obs}Py and $P(t_0)$ Py); and Py+A indicates sodium [1-^{13}C]pyruvate (Py) after hydrolysis with NaOH and ascorbate (P_{obs}Py+A and $P(t_0)$ Py+A). The observed hyperpolarization levels (P_{obs}PyE, P_{obs} Py and P_{obs} Py+A) are an average of at least three experiments.

Discussion

The ^{1}H-NMR spectra of the parahydrogen gas, acquired at the end of the *par*ahydrogenation reaction, show that significant para-enrichment loss occurs during in the time course of the reaction. It is known that a catalyst is necessary for parahydrogen to be converted and that the reversible coordination of the hydrogen molecule to a metal complex makes this a quick process [28]. However, the catalytic cycle at the used Rhodium complex does not imply hydrogen molecule exchange at the metal centre. The unsaturated substrate is coordinated to the metal complex before, the hydrogen molecule enters the coordination sphere and is irreversibly transferred to the product. Minimal (if any) para-ortho conversion can therefore be expected, using this kind of hydrogenation catalyst [28].

The substantial para-ortho conversion observed in the hydrogen gas ^{1}H-NMR spectra may be attributed to the presence of free Rhodium (both Rh^{2+} and Rh^{0}), that derives from partial catalyst degradation. In order to validate this hypothesis, ^{31}P-NMR spectra of the catalyst containing solution were acquired before and after the activation. It was observed that, after diene hydrogenation, the ^{31}P signal that corresponds to the coordinated ligand (see S.I.) was found to be only about 20% of the total ^{31}P-NMR signal and strong free phosphine and phosphine oxide absorption was detected. This means that a significant portion of the catalyst decomposes, under these experimental conditions, and that other Rh(II) and Rh(0) complexes are formed in

the reaction mixture. Moreover, the accurate washing of the reaction vessel, using a hot concentrated acidic solution to completely remove metal traces, was also found to be useful in removing any other sources of paramagnetic metal ions that may reduce polarization level.

Mixing between the singlet state (parahydrogen state), and the triplet states occurs in the hydrogenation intermediates, when parahydrogen is coordinated with the catalyst. This contributes to the depletion of parahydrogen state population and to consequent polarization loss.

Although the catalytic cycle operated by the $[Rh(diphos)]^+$ complexes works in such a way that reaction intermediates lifetimes are minimized compared with other homogeneous hydrogenation complexes [29], the mixing of the para-ortho states still occurs in hydrogenation intermediates [36]. We suggest that this may be the reason why only around 24% hyperpolarization was actually found on parahydrogen protons in ALTADENA experiments (nascent ^1H hyperpolarization: $P(t_0)$ ^1H). ^1H hyperpolarization might, in principle correspond to the para-enrichment of hydrogen if the hydrogenation catalyst was able to facilitate the addition of the pure singlet state to the substrate.

An important achievement is the beneficial role played by ascorbate. The ^{13}C polarization of [1-^{13}C]pyruvate, back calculated to time zero ($P(t_0)$), was 9.5% while the ^{13}C polarization of the allyl ester ($P(t_0)$) was 10.5%. It can therefore be stated that ^{13}C hyperpolarization is almost completely maintained during the hydrolysis and phase extraction steps.

It must also be highlighted that manual hydrolysis work-up takes approximately 40 s, during which time substantial hyperpolarization (about 50%) is lost, caused by relaxation processes.

Conclusions

The results reported show that ^{13}C hyperpolarization on the allyl ester of [1-^{13}C]pyruvate, following to *para*hydrogenation and MFC, was increased from about 2%, initially reported for the PHIP-SAH ester derivatives [31], to 5%.

Several steps have been improved. It has been assessed that MFC allows to transfer about 40% of ^{1}H hyperpolarization ($P(t_0)$ on ^{1}H: 23.9 ± 3.3 %), observed in the ALTADENA experiments, to the ^{13}C carboxylate signal of allyl ester ($P(t_0)$ on ^{13}C of allyl pyruvate: 10.4 ± 1).

The addition of ascorbate, a scavenger of paramagnetic impurities, considerably improved the maintenance of hyperpolarization during the hydrolysis step, and decreased the relaxation rate of the hyperpolarized signal. In practice, the nascent polarization on [1-^{13}C]pyruvate ($P(t_0)$) was 9.4 ± 0.5% while the polarization level obtained on the ester ($P(t_0)$) was 10.4± 1%. This small loss may be ascribed to relaxation phenomena that occur at the interface between the organic and the aqueous phase during emulsion formation.

It must be noticed that around half of the nascent polarization ($P(t_0)$) is lost during the time delay (40-45 seconds) between the end of the hyperpolarization procedure (the end of the MFC) and the acquisition of the NMR spectrum. This suggests that a dedicated and automatic set-up might be able to reduce the time needed for the work-up passages, which are currently carried out manually, and lead to an increase in the observed polarization level. Furthermore, it has been shown that parahydrogen enrichment is considerably diminished, during the hydrogenation reaction, which is probably due to the formation of metal impurities in the hydrogenation mixture. Further studies into hydrogenation catalysis are therefore a necessity.

These observation provide important clues as to how this may be achieved and the polarization level on PHIP-SAH products increased.

Acknowledgements

The Italian Association for Cancer Research is gratefully acknowledged for financial support (AIRC, 2015 TRIDEO call). This work was also supported by the Consorzio Interuniversitario di Ricerca in Chimica dei Metalli nei Sistemi Biologici (C.I.R.C.M.S.B.).

We acknowledge the support and advices from Aspect Imaging scientists (Peter Bendel and Yoram Cohen).

References

[1] T.C. Eisenschmid, R.U. Kirss, P.P. Deutsch, S.I. Hommeltoft, R. Eisenberg, J. Bargon, R.G. Lawler, A.L. Balch, Para Hydrogen Induced Polarization in Hydrogenation Reactions, J. Am. Chem. Soc. 109 (1987) 8089–8091. doi:10.1021/ja00260a026.

[2] C.R. Bowers, D.P. Weitekamp, Parahydrogen and synthesis allow dramatically enhanced

nuclear alignment, J. Am. Chem. Soc. 109 (1987) 5541–5542. doi:10.1021/ja00252a049.
[3] J. Natterer, J. Bargon, Parahydrogen induced polarization, Prog. Nucl. Magn. Reson. Spectrosc. 31 (1997) 293–315.
[4] R. V Shchepin, A.M. Coffey, K.W. Waddell, E.Y. Chekmenev, Parahydrogen Induced Polarization of 1- 13 C-Phospholactate- d 2 for Biomedical Imaging with >30,000,000-fold NMR Signal Enhancement in Water, Anal. Chem. 86 (2014) 5601–5605. doi:10.1021/ac500952z.
[5] E.Y. Chekmenev, J. Hövener, V.A. Norton, K. Harris, L.S. Batchelder, P. Bhattacharya, B.D. Ross, D.P. Weitekamp, PASADENA hyperpolarization of succinic acid for MRI and NMR spectroscopy, J. Am. Chem. Soc. 130 (2008) 4212–4213. doi:10.1021/ja7101218.
[6] K. Golman, O. Axelsson, H. Johannesson, S. Månsson, C. Olofsson, J. ~S. Petersson, Parahydrogen-induced polarization in imaging: Subsecond C-13 angiography, Magn. Reson. Med. 46 (2001) 1–5.
[7] L.E. Olsson, C.M. Chai, O. Axelsson, M. Karlsson, K. Golman, J.S. Petersson, MR coronary angiography in pigs with intraarterial injections of a hyperpolarized 13C substance, Magn. Reson. Med. 55 (2006) 731–737. doi:10.1002/mrm.20847.
[8] J.-B. Hövener, E.Y. Chekmenev, K.C. Harris, W.H. Perman, T.T. Tran, B.D. Ross, P. Bhattacharya, Quality Assurance of PASADENA Hyperpolarization for Carbon-13 Biomolecules, Magn. Reson. Mater. Phys. 22 (2009) 123–34. doi:10.1007/s10334-008-0154-y.
[9] A.M. Coffey, R. V. Shchepin, M.L. Truong, K. Wilkens, W. Pham, E.Y. Chekmenev, Open-source automated parahydrogen hyperpolarizer for molecular imaging using 13C metabolic contrast agents, Anal. Chem. 88 (2016) 8279–8288. doi:10.1021/acs.analchem.6b02130.
[10] J.H. Ardenkjaer-Larsen, B. Fridlund, A. Gram, G. Hansson, L. Hansson, M.H. Lerche, R. Servin, M. Thaning, K. Golman, Increase in signal-to-noise ratio of > 10,000 times in liquid-state NMR., Proc. Natl. Acad. Sci. U. S. A. 100 (2003) 10158–63. doi:10.1073/pnas.1733835100.
[11] K. Golman, R. in 't Zandt, M. Thaning, Real-time metabolic imaging., Proc. Natl. Acad. Sci. U. S. A. 103 (2006) 11270–5. doi:10.1073/pnas.0601319103.
[12] K.M. Brindle, Imaging Metabolism with Hyperpolarized ^{13}C-Labeled Cell Substrates, J. Am. Chem. Soc. 137 (2015) 6418–6427. doi:10.1021/jacs.5b03300.
[13] E.M. Serrão, K.M. Brindle, Potential Clinical Roles for Metabolic Imaging with Hyperpolarized [1-(13)C]Pyruvate, Front. Oncol. 6 (2016) 59. doi:10.3389/fonc.2016.00059.
[14] K. Golman, R.I.T. Zandt, M.H. Lerche, R. Pehrson, J.H. Ardenkjaer-Larsen, Metabolic imaging by hyperpolarized 13C magnetic resonance imaging for in vivo tumor diagnosis., Cancer Res. 66 (2006) 10855–60. doi:10.1158/0008-5472.CAN-06-2564.
[15] K. Golman, J.S. Petersson, P. Magnusson, E. Johansson, P. Åkeson, C.M. Chai, G. Hansson, S. Månsson, Cardiac metabolism measured noninvasively by hyperpolarized 13C MRI, Magn. Reson. Med. 59 (2008) 1005–1013. doi:10.1002/mrm.21460.
[16] C.H. Cunningham, J.Y.C. Lau, A.P. Chen, B.J. Geraghty, W.J. Perks, I. Roifman, G.A. Wright, K.A. Connelly, Hyperpolarized 13C Metabolic MRI of the Human Heart: Initial Experience, Circ. Res. 119 (2016) 1177–1182. doi:10.1161/CIRCRESAHA.116.309769.
[17] Y. Xu, S. Ringgaard, C. Østergaard Mariager, L. Bonde Bertelsen, M. Schroeder, H. Qi, C. Laustsen, H. Stødkilde-Jørgensen, Hyperpolarized 13 C Magnetic Resonance Imaging Can Detect Metabolic Changes Characteristic of Penumbra in Ischemic Stroke, Tomography. 3 (2017) 67–73. doi:10.18383/j.tom.2017.00106.
[18] F. Reineri, T. Boi, S. Aime, ParaHydrogen Induced Polarization of 13C carboxylate resonance in acetate and pyruvate, Nat. Commun. 6 (2015) 5858. doi:10.1038/ncomms6858.
[19] A.E. Cavallari, C. Carrera, S. Aime, E. Cavallari, C. Carrera, P.S. Aime, F. Reineri, C-MR Hyperpolarization of Lactate using ParaHydrogen and metabolic transformation in vitro ., Chem. — A Eur. J. (2017) 1200–1204. doi:10.1002/chem.201605329.
[20] R. V Shchepin, D.A. Barskiy, A.M. Coffey, I. V. Manzanera Esteve, E.Y. Chekmenev, Efficient Synthesis of Molecular Precursors for Para-Hydrogen-Induced Polarization of Ethyl Acetate-1-13C and beyond, Angew. Chemie - Int. Ed. 55 (2016) 6071–6074. doi:10.1002/anie.201600521.

[21] L.T. Kuhn, J. Bargon, Topics in Current Chemistry, in: J. Bargon (Ed.), Situ NMR Methods Catal., Springer, Berlin-Heidelberg, 2007: pp. 25–68. doi:10.1007/128_016.
[22] M. Plaumann, U. Bommerich, T. Trantzschel, D. Lego, S. Dillenberger, G. Sauer, J. Bargon, G. Buntkowsky, J. Bernarding, Parahydrogen-Induced Polarization Transfer to 19 F in Perfluorocarbons for 19 F NMR Spectroscopy and MRI**, Chem. - A Eur. J. 19 (2013) 6334–6339. doi:10.1002/chem.201203455.
[23] M. Goldman, H. Jóhannesson, Conversion of a proton pair para order into C-13 polarization by rf irradiation, for use in MRI, Comptes Rendus Phys. 6 (2005) 575–581. doi:10.1016/j.crhy.2005.03.002.
[24] M. Haake, J. Natterer, J. Bargon, Efficient NMR pulse sequences to transfer the parahydrogen-induced polarization to hetero nuclei, J. Am. Chem. Soc. 118 (1996) 8688–8691. doi:10.1021/ja960067f.
[25] S. Kadlecek, K. Emami, M. Ishii, R. Rizi, Optimal transfer of spin-order between a singlet nuclear pair and a heteronucleus, J. Magn. Reson. 205 (2010) 9–13. doi:10.1016/j.jmr.2010.03.004.
[26] S. Bär, T. Lange, D. Leibfritz, J. Hennig, D. Von Elverfeldt, J.B. Hövener, On the spin order transfer from parahydrogen to another nucleus, J. Magn. Reson. 225 (2012) 25–35. doi:10.1016/j.jmr.2012.08.016.
[27] H. Jóhannesson, O. Axelsson, M. Karlsson, Transfer of para-hydrogen spin order into polarization by diabatic field cycling, Comptes Rendus Phys. 5 (2004) 315–324. doi:10.1016/j.crhy.2004.02.001.
[28] J.B. Hövener, E.Y. Chekmenev, K.C. Harris, W.H. Perman, L.W. Robertson, B.D. Ross, P. Bhattacharya, PASADENA hyperpolarization of 13C biomolecules: equipment design and installation., MAGMA. 22 (2009) 111–121. doi:10.1007/s10334-008-0155-x.
[29] K.W. Waddell, A.M. Coffey, E.Y. Chekmenev, In Situ Detection of PHIP at 48 mT : Demonstration Using a Centrally Controlled Polarizer, (2011) 153–157.
[30] J. Agraz, A. Grunfeld, D. Li, K. Cunningham, C. Willey, R. Pozos, S. Wagner, LabVIEW-based control software for para-hydrogen induced polarization instrumentation, Rev. Sci. Instrum. 85 (2014). doi:10.1063/1.4870797.
[31] E. Cavallari, C. Carrera, T. Boi, S. Aime, F. Reineri, Effects of Magnetic Field Cycle on the Polarization Transfer from Parahydrogen to Heteronuclei through Long-Range J-Couplings, J. Phys. Chem. B. 119 (2015) 10035–10041. doi:10.1021/acs.jpcb.5b06222.
[32] A.B. Schmidt, S. Berner, W. Schimpf, C. Müller, T. Lickert, N. Schwaderlapp, S. Knecht, J.G. Skinner, A. Dost, P. Rovedo, J. Hennig, D. von Elverfeldt, J.-B. Hövener, Liquid-state carbon-13 hyperpolarization generated in an MRI system for fast imaging, Nat. Commun. 8 (2017) 14535. doi:10.1038/ncomms14535.
[33] B. Feng, A.M. Coffey, R.D. Colon, E.Y. Chekmenev, K.W. Waddell, A pulsed injection parahydrogen generator and techniques for quantifying enrichment, J. Magn. Reson. 214 (2012) 258–262. doi:10.1016/j.jmr.2011.11.015.
[34] M.G. Pravica, D.P. Weitekamp, Net Nmr Alignment by Adiabatic Transport of Para-Hydrogen Addition-Products to High Magnetic-Field, Chem. Phys. Lett. 145 (1988) 255–258. wos:A1988N154500001.
[35] P. Miéville, P. Ahuja, R. Sarkar, S. Jannin, P.R. Vasos, S. Gerber-Lemaire, M. Mishkovsky, A. Comment, R. Gruetter, O. Ouari, P. Tordo, G. Bodenhausen, Scavenging free radicals to preserve enhancement and extend relaxation times in NMR using dynamic nuclear polarization, Angew. Chemie - Int. Ed. 49 (2010) 6182–6185. doi:10.1002/anie.201000934.
[36] J. Natterer, O. Schedletzky, J. Barkemeyer, J. Bargon, S. Glaser, Investigating catalytic processes with parahydrogen: evolution of zero-quantum coherence in AA'X spin systems, J. Magn. Reson. 133 (1998) 92–7. doi:10.1006/jmre.1998.1421.
[37] M. Goldman, H. Jóhannesson, Conversion of a proton pair para order into 13C polarization by rf irradiation, for use in MRI, Comptes Rendus Phys. 6 (2005) 575–581. doi:10.1016/j.crhy.2005.03.002.
[38] M. Goldman, H. Johannesson, O. Axelsson, M. Karlsson, Design and implementation of 13C hyper polarization from para-hydrogen, for new MRI contrast agents, Comptes Rendus Chim. 9 (2006) 357–363. doi:10.1016/j.crci.2005.05.010.